Eur. Phys. J. Special Topics **224**, 659–686 (2015)
© EDP Sciences, Springer-Verlag 2015
DOI: 10.1140/epjst/e2015-02398-6

THE EUROPEAN PHYSICAL JOURNAL SPECIAL TOPICS

Regular Article

Soil radon (^{222}Rn) monitoring at Furnas Volcano (São Miguel, Azores): Applications and challenges

C. Silva[1,2,a], T. Ferreira[2], F. Viveiros[2], and P. Allard[3]

[1] Centro de Vulcanologia e Avaliação de Riscos Geológicos, Universidade dos Açores, Ponta Delgada, Portugal
[2] Centro de Informação e Vigilância Sismovulcânica dos Açores, Universidade dos Açores, Ponta Delgada, Portugal
[3] Institut de Physique du Globe de Paris, IPGP, Paris, France

Received 2 March 2015 / Received in final form 23 April 2015
Published online 10 June 2015

Abstract. A soil ^{222}Rn continuous monitoring test was performed in three sampling points inside Furnas Volcano caldera and ^{222}Rn concentration varied between 0 and 153000 Bq/m^3. Multivariate regression and spectral analyses were applied to the time series registered in order to understand and filter the influence of external factors on soil ^{222}Rn concentration and to recognise anomalies correlated with deep processes. The regression models show that barometric pressure, soil water content, soil temperature, soil CO_2 flux, air temperature, relative air humidity and wind speed are the statistical meaningful variables explaining between 15.8% and 73.6% of ^{222}Rn variations. Spectral analysis allowed to identify seasonal variations and daily variations associated with one cycle per day on winter months only in one of the monitored sites. This diurnal variation is correlated with air temperature, relative air humidity and wind speed cycles. The change in the location of the sampling points was caused by both artificial and natural constrains. On the three monitoring sites, after a period of continuous register, a sudden drop on the ^{222}Rn concentration values was observed and the cause is still under debate. The work performed can be applied for seismovolcanic monitoring and for public health risk assessment.

1 Introduction

The Azores archipelago is formed by nine volcanic islands located on the North Atlantic Ocean, where the North American, Eurasian and African tectonic plates meet. Due to this particular geological setting the Azorean islands have been affected by several destructive earthquakes and volcanic eruptions since its settlement. São Miguel Island, the largest and more densely populated island of the archipelago, is formed by basaltic rift zones and three main quiescent central volcanoes: Sete Cidades,

[a] e-mail: Catarina.PP.Silva@azores.gov.pt

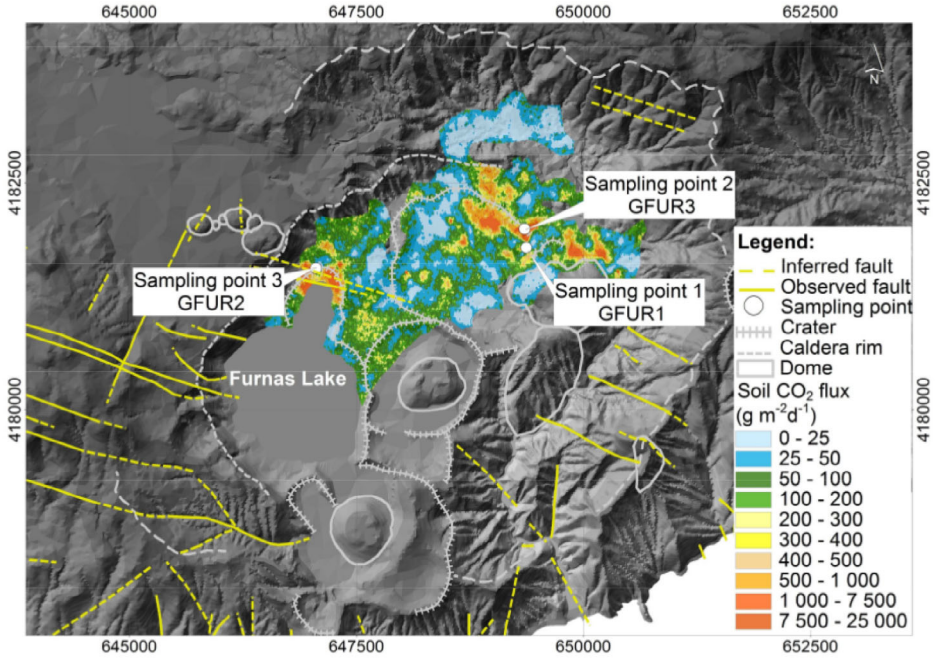

Fig. 1. Furnas Volcano elevation model, E-type soil CO_2 flux map [5], main volcano-tectonic structures [5 and references therein] and the location of the sampling points in Furnas caldera, where the soil ^{222}Rn continuous monitoring test was performed (UTM-WGS84, zone 26S). Sampling points 1, 2 and 3 correspond also to the location of GFUR1, GFUR3, and GFUR2 soil CO_2 flux monitoring stations, respectively.

Fogo and Furnas (Appendix A, Fig. A1). Furnas Volcano is a trachytic central volcano with caldera, inside which at least 10 eruptions occurred in the last 5000 years, and the last two occurred after the settlement (1439-43; 1630) [1,2]. At present, several secondary manifestations of volcanism can be observed at this volcano, comprising four main fumarolic fields, several thermal and cold CO_2-rich springs. The hydrothermal system that feeds the intracaldera fumaroles is located at a depth of 100–200 m with temperatures ranging from 160 to 180 °C [3,4]. Since the early nineties anomalous soil diffuse degassing zones (CO_2 and ^{222}Rn) were also identified (Fig. 1) [5–10]. Two villages are located in the Furnas Volcano geographical area: Furnas Village located inside the caldera and Ribeira Quente Village located on the South flank, both of which are placed over degassing areas [5–10].

The study of soil ^{222}Rn diffuse degassing (mapping and continuous monitoring) can give important information about the volcanic activity [11–29]. ^{222}Rn is a radioactive, colourless and odourless noble gas that results from the radioactive decay chain of uranium (^{238}U). Due to its short half-life (3.82 days), the ^{222}Rn measured at small depth is normally related both with a shallow source within the volcanic system or with the soils and rocks nearby the sampling point. However, in presence of an efficient transport agent, ^{222}Rn from magma can also reach the surface [30]. ^{222}Rn anomalies on volcanic systems can be related to an increase of the ground permeability (i.e. seismic activity), an increase in the velocity of ground gas migration (presence of carrier gases), an increase in the temperature (releasing the ^{222}Rn dissolved in the hydrothermal system or present in the rocks), or with release of ^{222}Rn due to a magma intrusion [11]. Despite the correlations established between ^{222}Rn emissions and volcanic eruptions, several works have also correlated this gas with seismic activity on fault zones [31–35]. While a strict and clear relation between ^{222}Rn and

seismicity is still under debate, correlations between ^{222}Rn anomalies and volcanic eruptions seem to be better established as shown, for instance, on Karymsky [36], Kilauea [11,12], Cerro Negro [13], Popocatepetl [15–17], Galeras [14], Vulcano [37], Etna [18–25], and Stromboli [26–29] volcanoes. Soil ^{222}Rn variations can however be influenced by external variables that can interfere with ^{222}Rn release and transport near the surface [13]. Based on this, understanding and filtering out the influence of external parameters on soil ^{222}Rn variation is fundamental to identify eventual ^{222}Rn anomalies related with deep processes.

The main purpose of this work is to study soil ^{222}Rn temporal variations on a quiescent volcanic system and to define ^{222}Rn background level for Furnas Volcano in order to recognize future signs of reactivation. Considering that several factors may interfere with soil ^{222}Rn concentrations, despite the volcanic activity itself, information about environmental variables and seismic activity (that can increase the permeability of the volcanic system [11,12]) at Furnas Volcano will be presented and discussed. Considering that CO_2 can act as a carrier gas transporting ^{222}Rn until the surface [38–43], information about its temporal variations will also be included in the data analyses. The importance of accounting with CO_2 variations to understand the state of activity of a volcano is also supported by the fact that CO_2, besides water vapour, is the major gas species in both volcanic fluids and magmas, and it is one of the first gases released from the magma, fact that is fundamental for volcanic monitoring studies [30,38,44–46].

2 Methodology

Soil ^{222}Rn measurements were performed with a solid state alpha detector, the RAD7 equipment, (Durridge Company Inc.). This equipment was programmed to run in auto mode allowing to calculate the ^{222}Rn concentration focusing on the ^{218}Po alpha peak during the first three hours and, after that, on both ^{218}Po and ^{214}Po alpha peaks. The measurements were performed in continuous cycles of 60 minutes, pumping in air from depth of around 60 cm. The pump flow rate was 0.5 L/minute. The pump, in auto mode, switches on for four minutes at the beginning of a new cycle, and then runs one minute in every five until the end of the cycle. However, if the humidity in the sampling cell is above 10% the pump stays on to allow the cell to dry out.

Data acquired by the permanent soil CO_2 flux (GFUR1, GFUR2, and GFUR3) (Fig. 1), that belong to the CVARG/CIVISA permanent monitoring network, were used to recognize the influence of environmental variables and soil CO_2 flux on the soil ^{222}Rn concentration. Soil CO_2 fluxes were measured using the accumulation chamber method and the results obtained were already analyzed and discussed on previous works [47–49]. These stations are located in the vicinities of the soil ^{222}Rn sampling points and give also information on environmental parameters, namely: barometric pressure, rainfall, wind speed, air temperature, relative air humidity, soil temperature, and soil water content. Technical characteristics of the sensors used are available in Appendix B (Table B1).

We are aware that results obtained through the use of different methodologies to measure soil gases (soil gas concentration vs soil gas flux) may show some differences, essentially correlated with the permeability of the superficial layers of the soil; however previous studies performed at Furnas Volcano showed similar spatial distribution of the anomalous degassing areas using both soil CO_2 concentrations measured at 60 cm depth [7,8] and soil CO_2 fluxes measured at soil surface with the accumulation chamber [5]. This evidence suggests that measurements performed at the surface reflect what is happening in the subsurface soil layers. The study of the

relation between ^{222}Rn and other geochemical/physical parameters (as CO_2 or soil temperature) is quite important, since the presence of CO_2 and/or temperature indicates the presence of advective and/or convective transport types, and one may infer that the ^{222}Rn that is being measured was transported from longer distances and therefore can be an indicator of the processes that are happening at deeper zones [11,13,38,39,43,50,51].

The data obtained was analysed statistically using both spectral analyses and stepwise multivariate regression in order to understand and filter the statistical influence of those factors on soil ^{222}Rn concentration.

Spectral analysis was applied using the Tsoft software, version 2.1.15 [52,53]. This software uses Fast Fourier Transform (FFT) to calculate the spectrum that decomposes a time domain signal into a signal expressed in the frequency domain. Since each point depends on all points of the filtered channel, the results are influenced by the limitations in time of the data series and by the presence of gaps [52]. A period with less data gaps was selected to apply the spectral analysis, being the gaps corrected. When only one hour of data was missing the value was interpolated being calculated the average of the previous and next values in the time series. When two or more hours of data were missing, the 24 hours of data related with that day (from 00:00 to 23:00) were removed from all the time series of the variables under study. This assures that a complete 24 hours period per day is always present and allows comparing the different time series. To identify daily cyclic variations, the spectrum of the time series was calculated based on FFT, being selected an increase interval of 3600 seconds and the Hanning function that forces the endpoints to zero reducing the spectral leakage [54]. When daily variations were identified, Transfer Function was applied between two selected time series (soil ^{222}Rn concentration and environmental variables) allowing to assess amplitude ratios, time delay between the time series (phase) and coefficients of correlation for the different frequencies [53]. Using the Moving Window Spectrum, the spectrogram was computed and frequency was plotted against time, being the colours representative of the amplitudes of the frequency. The spectrogram allows to identify seasonal variations [52].

Stepwise multivariate regression analysis was also applied to the time series with the software SPSS® (Statistical Packages for the Social Sciences), version 16. In this analysis soil ^{222}Rn concentration was considered the dependent variable and environmental parameters, as well as soil CO_2 flux, were the independent variables, according to the equation 1 [55,56].

$$Y_i = B_0 + B_1X_1 + B_2X_2 + \ldots + B_kX_k + \varepsilon_i, \qquad i = 1, 2, \ldots n. \tag{1}$$

The regression model included only the independent variables that were significant according to the t test (significance < 0.01), and which increased the adjusted R^2 by more than 1%. The application of regression models to time series requires a normally distributed population. Geochemical data in general do not follow normal distribution and have to be transformed [55]. In the present case, even the transformed data do not follow a log-normal distribution (Fig. 2). However, a pattern on the distribution of the data in the three sampling sites was recognised: a group of data with low values (GLV), a group of data with intermediate values (GIV) and a group of data with high values (GHV). The regression analysis was therefore applied separately to each of the groups, whether the data follow a normal or log-normal distribution. The application of regression analysis also requires a non-multicollinearity between the independent variables, what can be checked calculating the variance inflation factor (VIF). Variables with VIF values higher than 10 were excluded [56].

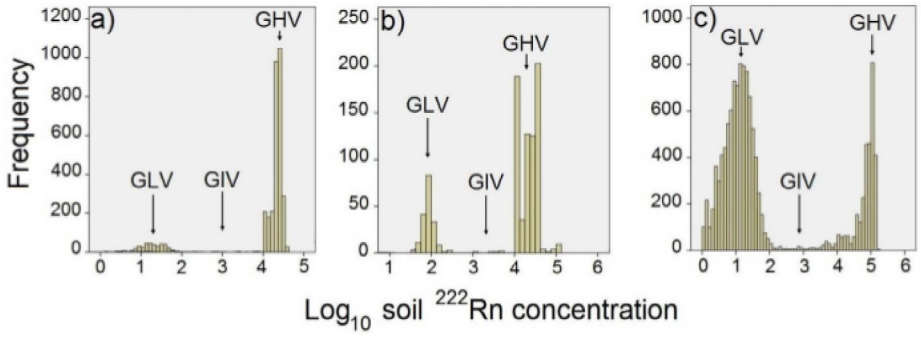

Fig. 2. Histograms of the log-transformed soil ^{222}Rn data on the three sampling points: a) Sampling point 1 – Furnas Thermal Center, b) Sampling point 2 – Furnas Village Fumarolic Field, and c) Sampling point 3 – Furnas Lake Fumarolic Field. Three groups of data identified: GLV – Group of data with low values, GIV – Group of data with intermediate values, and GHV – Group of data with high values.

3 Sampling sites

A soil ^{222}Rn continuous monitoring test was performed in three sampling points inside Furnas caldera between 2005 and 2011 (Fig. 1). The sampling points were selected taking into account various criteria: (1) possible transport type (advective or convective) that allows to measure ^{222}Rn originated from deeper zones, (2) presence of fumarolic fields, (3) the different volcano-tectonic structures present at Furnas Volcano [2,57,58], and (4) the soil diffuse degassing maps (^{222}Rn and CO_2) performed in previous works [5,7–10]. The change in the location of the sampling sites was due to both artificial and natural constrains.

On sampling point 1 – Furnas Thermal Center, soil ^{222}Rn concentration continuous measurements started on August 2005 and lasted during five months. This sampling point was located in a garden that belongs to the Furnas Thermal Center, in an adjacent area to Furnas Village fumarolic field. Technical problems during download of the data were responsible for the gap registered between 21st September and 3rd October 2005. On January 2006, the ^{222}Rn equipment was removed from this sampling site due to the rebuilding of the Furnas Thermal Center. On sampling point 2 – Furnas Village Fumarolic Field, soil ^{222}Rn concentration continuous measurements were performed during only one month, between 23rd January and 29th February 2008. This short sampling period was related with the presence of hydrogen sulfide (H_2S) that damaged the electronic components of the equipment. On sampling point 3 – Furnas Lake Fumarolic Field, soil ^{222}Rn concentration continuous measurements were performed in the vicinity of the Furnas Lake Fumarolic Field, during approximately two years, between January 2009 and February 2011. The gaps registered were the result of technical problems in the detector. The exception was the period between 7th February and 13th April 2009, which resulted from lack of power supply since the solar panel was stolen.

4 Variation on the time domain

On sampling point 1, soil ^{222}Rn concentration continuous measurements were performed between 18th August 2005 and 16th January 2006 and the measured values varied between 0 and 39200 Bq/m^3 (Fig. 3a). Soil ^{222}Rn concentration values varied

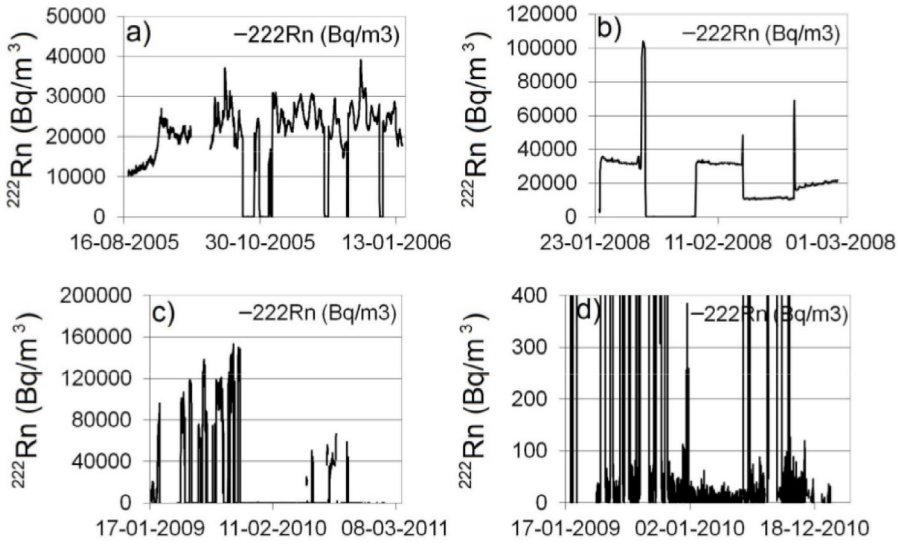

Fig. 3. Soil ^{222}Rn concentration temporal variations on the sampling points: a) sampling point 1 – Furnas Thermal Center, b) sampling point 2 – Furnas Village Fumarolic Field, c) sampling point 3 – Furnas Lake Fumarolic Field total scale, and d) sampling point 3 – Furnas Lake Fumarolic Field enlarged scale (0–400 Bq/m^3).

between 33 and 104000 Bq/m^3 on sampling point 2 (Fig. 3b). On sampling point 3 soil ^{222}Rn concentration continuous measurements were performed from 20th January 2009 to 1st February 2011 and varied between 0 and 153000 Bq/m^3 (Fig. 3c and d). Descriptive statistics of soil ^{222}Rn concentration, soil CO_2 flux, and soil temperature are displayed in Appendix B (Table B2). The sampling point 1 is located in an area without thermal anomaly, while sampling points 2 and 3 are located in soil temperature anomalous zones.

The analysis of the temporal variation of soil ^{222}Rn concentration, soil CO_2 flux, and the environmental parameters suggests a relation between soil ^{222}Rn concentration and some of the variables under study (Fig. 4). On sampling point 1 soil ^{222}Rn concentration variations seem to be correlated with barometric pressure, rainfall, and soil water content, while on sampling point 3, this gas variation seems to be related with wind speed and air temperature. Soil CO_2 flux seems to correlate with soil ^{222}Rn concentration on both sampling points. The short sampling period on sampling point 2, did not allow recognizing any relation between soil ^{222}Rn concentration and the variables under study. Spectral and multivariate regression analyses were applied to the time series of the variables under study to confirm statistically the relations observed. The analysis of the soil ^{222}Rn concentration temporal variation also allows to observe sudden drops and increases in the values registered on the three sampling sites (Fig. 3). A detail of this behaviour can be observed on Fig. 5. The changes observed occurred in a time interval of some hours, 4 or 5 hours, and correspond to a decrease rate of 29738 Bq/m^3.h and an increase rate of 17939 Bq/m^3.h. The cause of these sudden drops is still not clear (e.g. technical problems or local effect).

5 Variation on the spectral domain

Spectral analysis was applied, on sampling point 1, to the sampling period between 3rd October 2005 and 16th January 2006. The period selected corresponds, as stated

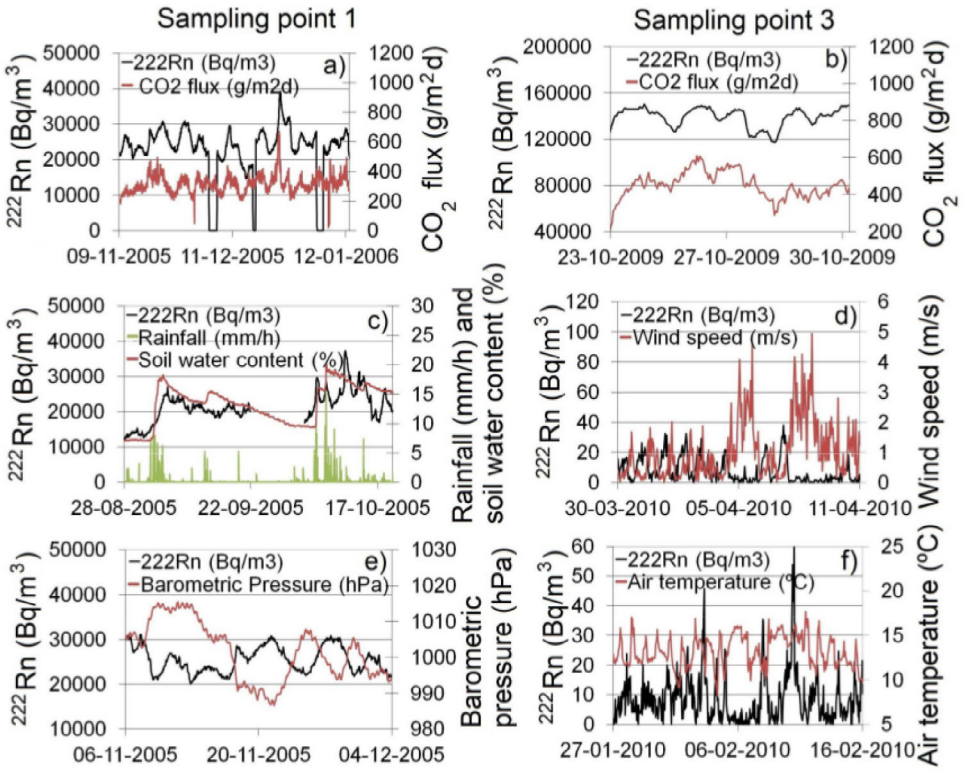

Fig. 4. Soil ^{222}Rn concentration, soil CO_2 flux and several environmental parameters (rainfall/soil water content, wind speed, barometric pressure, and air temperature) temporal variations on the sampling points 1- Furnas Thermal Center and 3- Furnas Lake Fumarolic Field, for different sampling periods.

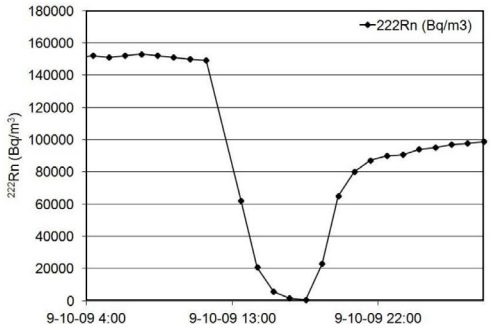

Fig. 5. Soil ^{222}Rn concentration on sampling point 3- Furnas Lake Fumarolic Field. Detail of the sudden decrease and increase of ^{222}Rn values.

before, to the period with less gaps in the time series. This analysis did not allow identifying daily cyclic variations (Fig. 6a). Due to the short sampling period, together with absence of periodicity, the spectrogram was not calculated. On sampling point 2, and as result of the short sampling period, spectral analysis was not applied to the data acquired.

The spectral analysis was applied, on sampling point 3, to the sampling period between 13th May 2009 and 20th November 2010, as it represents the period with less

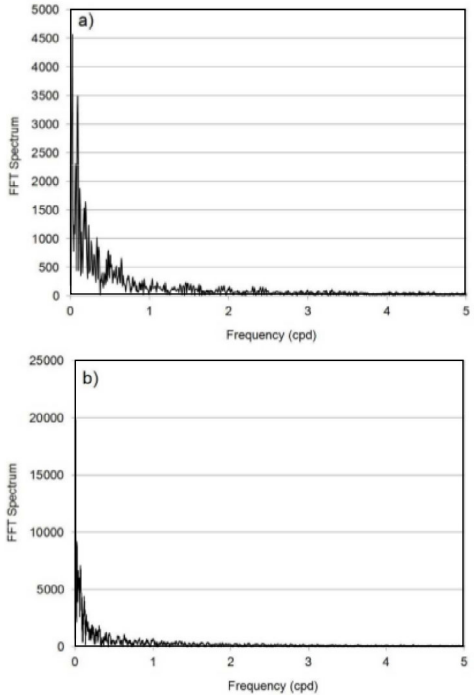

Fig. 6. Amplitude spectra of soil ^{222}Rn concentration temporal variation: a) on the sampling point 1- Furnas Thermal Center, for the period between 03-10-2005 and 16-01-2006, and b) on the sampling point 3- Furnas Lake Fumarolic Field, for the period between 13-05-2009 and 20-11-2010.

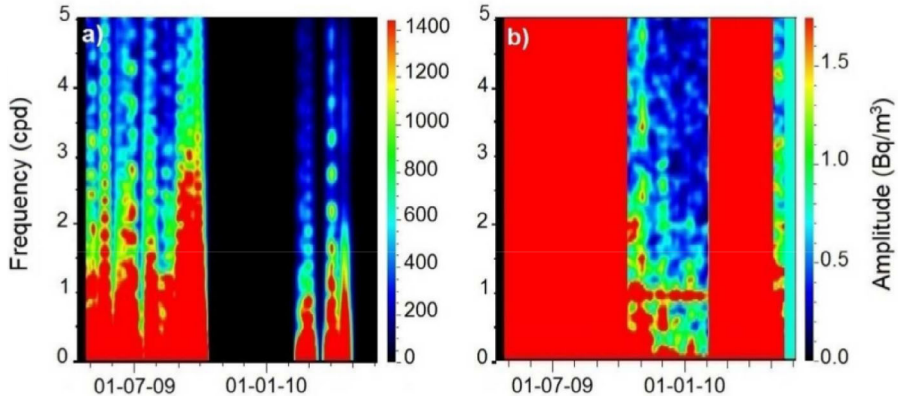

Fig. 7. Spectrogram of soil ^{222}Rn concentration temporal variation on the sampling point 3- Furnas Lake Fumarolic Field, for the period between 13-05-2009 and 20-11-2010: a) dry period, b) wet period (enlarged amplitude scale).

gaps in the time series. The spectrum calculated did not show daily cyclic variations (Fig. 6b). However, the spectrogram (Fig. 7) allowed to identify a seasonal behaviour (dry "summer" vs. wet "winter" seasons). This seasonal behaviour was confirmed by the spectra calculated (Fig. 8c and d), that did not show any daily cyclic variation for the dry period, but showed daily cyclic variations related with one cycle per

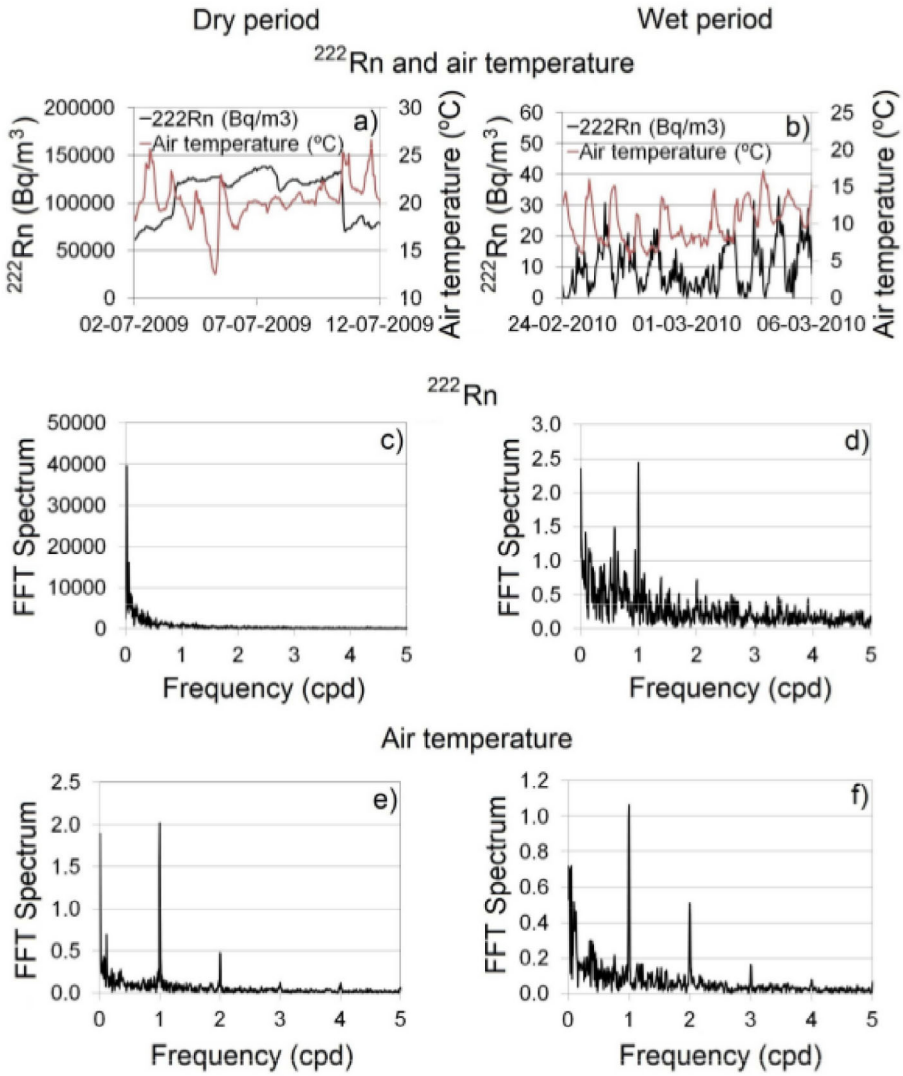

Fig. 8. Temporal variations and amplitude spectra of soil ^{222}Rn concentration and air temperature on the sampling point 3- Furnas Lake Fumarolic Field for the dry and wet period: a) soil ^{222}Rn concentration and air temperature temporal variation during 10 days on the dry and b) on the wet period, c) amplitude spectrum of soil ^{222}Rn concentration temporal variation on the dry (13-05-2009 to 31-10-2009) and d) on the wet period (01-11-2009 to 25-04-2010), e) amplitude spectrum of air temperature temporal variation on the dry (13-05-2009 to 31-10-2009) and f) on the wet period (01-11-2009 to 25-04-2010).

day (S1) for the wet period. The wet period comprises the months from November to April and this division was made taking into account both the spectrogram and the hydrological year [59]. The missing daily periodicity on the dry period cannot be associated with the treatment of the gaps since it was exactly the same for the dry and wet periods; in addition, parameters as air temperature, which are characterized by the presence of daily periodicities, show that periodicity on both periods (Fig. 8). On another hand a similar annual division was observed on the soil CO_2

Table 1. Correlation and time delay between the soil ^{222}Rn concentration and each of the meteorological variables, for the period between 01-11-2009 and 25-04-2010.

	Correlation coefficient	Delay (h)
Air temperature	0.95	∼12
Relative humidity	0.81	∼3
Wind speed	0.65	∼9

flux data obtained at this sampling point [6,48]. The coefficient of correlation and the time delay between soil ^{222}Rn concentration and the environmental parameters for the wet period (air temperature, relative air humidity, soil temperature, soil water content, barometric pressure, rainfall and wind speed) were calculated for one cycle per day variations using the Transfer Function and considering coefficients of correlation higher than 0.5. On this analysis, air temperature, relative air humidity and wind speed (Table 1) are the variables with coefficients of correlation higher than 0.5 with the soil ^{222}Rn concentration. Soil ^{222}Rn concentration shows a 12 hours delay in relation with air temperature, a 9 hours delay with wind speed and a 3 hours delay with relative air humidity. The low frequencies analysis allowed also to identify other periodic variations related with 340, 48, 25 and 15 days (Appendix A, Fig. A2).

6 Multivariate regression analysis and modelling

The histograms produced to apply stepwise multivariate regression allowed to recognize three different groups of data on each sampling point. Multivariate regression analysis was applied to each group, when the data of the group followed a normal or a log-normal distribution.

On sampling point 1 – Furnas Thermal Center, the three groups of data recognized were (Fig. 2): Group A1 (^{222}Rn values $\leq$ 8000 Bq/m^3), Group B1 (8000 Bq/m^3 $<$ ^{222}Rn values $\leq$ 16000 Bq/m^3), and Group C1 (^{222}Rn values $>$ 16000 Bq/m^3). The multivariate regression analysis applied to the group of data A1 (Appendix B, Table B3) allows identifying soil water content and soil temperature as the variables that influence soil ^{222}Rn variation. These variables show a negative correlation with soil ^{222}Rn concentration and have an explanatory power of 15.8% (adjusted R^2 sum). The variables that influence soil ^{222}Rn variation on group B1 are barometric pressure, soil temperature and soil water content. These variables explain 73.6% of the total soil ^{222}Rn variation (Appendix B, Table B3). Barometric pressure correlates inversely with soil ^{222}Rn concentration. Soil temperature and soil water content show a second-order polynomial function behaviour. Soil temperature has a positive correlation with soil ^{222}Rn concentration until 18.3°C, changing the correlation signal for negative above that value. In what concerns soil water content, a positive correlation is observed until 10.9%, changing the correlation signal to negative above that value. The VIF values are higher than 10 for soil temperature and (soil temperature)^2 and for soil water content and (soil water content)^2, however the multicollinearity is accepted in these cases, since it is in fact the same physical parameter that shows a second-order influence. The soil ^{222}Rn variation on group C1 is influenced by soil water content, soil CO_2 flux and soil temperature. These variables explain 40.5% of the total ^{222}Rn variation (Appendix B, Table B3). Soil water content and soil CO_2 flux express a positive correlation with soil ^{222}Rn concentration, while soil temperature shows a second-order polynomial function behaviour, positively influencing soil ^{222}Rn concentration until 17.6 °C, and negatively above that value. The VIF values are also accepted in this case, similarly to the above mentioned.

On sampling point 2 – Furnas Village Fumarolic Field, due to the limited data set, the multivariate regression analysis was applied only to recognize the influence of some of the parameters under study and not with the purpose of building a model. The groups of data identified on the histogram were (Fig. 2): Group A2 (^{222}Rn values $\leq$ 8000 Bq/m^3), Group B2 (8000 Bq/m^3 $<^{222}$Rn values $\leq$ 16 000 Bq/m^3), and Group C2 (^{222}Rn values $>$ 16000 Bq/m^3). This division is similar to the one defined in sampling point 1. Regression analysis was not applied to the group of data B2 due to the reduced number of observations. The multivariate regression analysis applied to the group of data A2 allowed identifying soil temperature, soil water content and wind speed as the variables that influence soil ^{222}Rn variation. These variables show a positive correlation with soil ^{222}Rn concentration, explaining 61.5% of the total variation (Appendix B, Table B4). On the group C2, the variables that influence soil ^{222}Rn variation are barometric pressure and air temperature. These variables explain 57.8% of the total ^{222}Rn variation (Appendix B, Table B4) and show a positive correlation with soil ^{222}Rn concentration.

On sampling point 3 – Furnas Lake Fumarolic Field, the groups of data identified were (Fig. 2): Group A3 (^{222}Rn values $\leq$ 8000 Bq/m^3), Group B3 (8000 Bq/m^3 $<^{222}$Rn values $\leq$ 50 000 Bq/m^3), and Group C3 (^{222}Rn values $>$ 50000 Bq/m^3). The multivariate regression analysis applied to the group of data A3 allows to identify soil temperature, wind speed, relative air humidity and soil CO_2 flux as the variables that influence soil ^{222}Rn variation. These variables explain 27% of the total variation observed (Appendix B, Table B5). Soil temperature, relative air humidity and soil CO_2 flux show a positive correlation with soil ^{222}Rn concentration, while wind speed shows a negative correlation. Multivariate regression analysis results are in agreement with the results of the spectral analysis applied to the wet period in what concerns relative air humidity and wind speed. The entire dataset of the wet period belongs to the group of data A3 ($\leq$ 8000 Bq/m^3). The multivariate regression analysis was applied to the group B3 not with the purpose of building an explicative model to soil ^{222}Rn variation, since the data do not follow a normal or a log-normal distribution, but to try to recognize the influence of some of the parameters under study. The statistically meaningful monitored variables that explain soil ^{222}Rn variation are wind speed and relative air humidity. The above mentioned variables show a negative correlation with soil ^{222}Rn variation, explaining 12% of the total variation (Appendix B, Table B5). The soil ^{222}Rn variation on group C3 is influenced by soil water content, soil temperature and soil CO_2 flux. These variables explain 50.4% of the total soil ^{222}Rn variation (Appendix B, Table B5). Soil CO_2 flux and soil water content correlate positively with soil ^{222}Rn concentration, while soil temperature shows a second-order polynomial function behaviour with a positive correlation with soil ^{222}Rn concentration until 24.2 °C, and negative correlation above that value. Similarly to the referred previously, the VIF values are also accepted in this case.

The multivariate regression analysis applied to the different datasets identified allowed the construction of models (Eqs. (2), (3), and (4) in Fig. 9) and the graphic projection of the predicted and residuals soil ^{222}Rn values according to the models proposed (Fig. 9). The residuals represent the variation that cannot be explained by the models and can be related either with deep variations or with external variables that are not being introduced in the multivariate regression analysis.

7 Radon anomalies (residuals) and seismic activity

During the sampling period, Furnas Volcano did not show signs of reactivation (e.g. magma intrusion), but several seismic events were registered on the study area and,

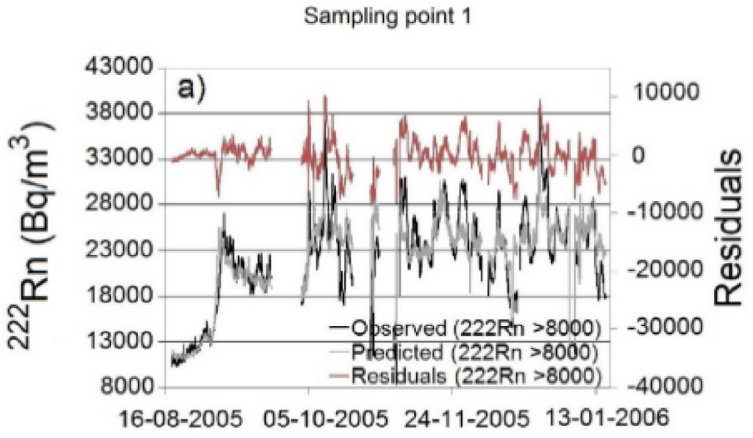

$$B1\text{-}\left[^{222}Rn\right]=144631.14-209.94\times BarP-214.87\times\left(T_{soil}\right)^{2}+1998.03\times WC_{soil}-99.07\times\left(WC_{soil}\right)^{2}+7859.48\times T_{soil} \quad (2)$$

$$C1\text{-}\left[^{222}Rn\right]=-31700.94-893.71\times WC_{soil}+365.03\times CO_{2\_flux}-122.27\times\left(T_{soil}\right)^{2}+4249.67\times T_{soil} \quad (3)$$

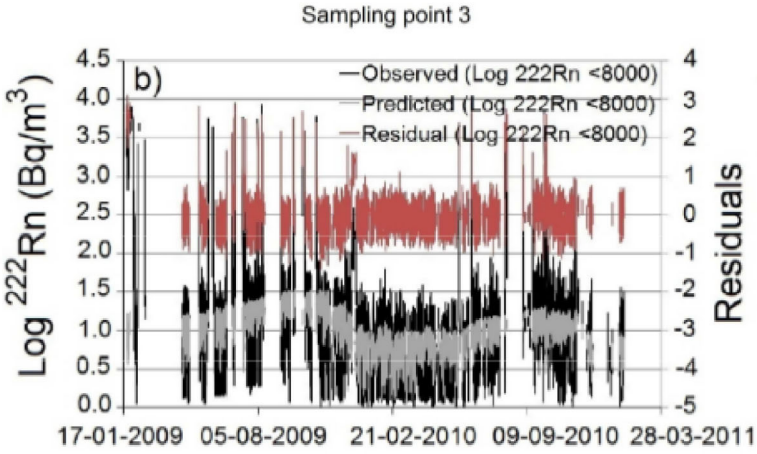

$$A3\text{-}Log_{10}\left[^{222}Rn\right]=-0.44+0.04\times T_{soil}-0.13\times W_{speed}+0.01\times RH_{air}+0.01\times CO_{2\_flux} \quad (4)$$

Fig. 9. Observed, predicted and residuals of soil ^{222}Rn values on sampling points 1 and 3: a) Groups B1 and C1 calculated with the models proposed on Eqs. (2) and (3), respectively, and b) Group A3 calculated with the model proposed on Eq. (4): BarP – barometric pressure, T_{soil} – soil temperature, WC_{soil} – soil water content, CO_{2_flux} – soil CO_2 flux, W_{speed} – wind speed, and RH_{air} – relative air humidity.

therefore, this information was included on the analyses of the soil ^{222}Rn data. The calculated residuals of the multivariate regression analysis were used to try to identify anomalies that could be related with seismic events and thus with an increase on the permeability of the system. The average (μ) and the standard deviation (σ) of the residuals were calculated and the values that fell outside the defined variability band ($\mu \pm 2\sigma$) are considered anomalous [33,48,60,61].

During the measurements performed between 18$^{\text{th}}$ August 2005 and 16$^{\text{th}}$ January 2006, on sampling point 1 – Furnas Thermal Center, 924 seismic events were recorded on Furnas Volcano area with duration magnitudes (Md) that

varied between 0.4 and 3.8 (CVARG/CIVISA, http://www.cvarg.azores.gov.pt/paginas/sismicidade.aspx). Duration magnitudes were calculated by measuring the duration, time in seconds, from the onset of the first P-arrival to the point at which the coda drops below the background level and applying the empirical relation of Lee et al. [62]. The advantages of using duration magnitudes are that the signal duration does not depend on the distance from the source to the station until 100 Km or on the sensitivity of the instrument, allowing calculating duration magnitudes on any station without epicentral distance factors in most volcanic monitoring circumstances [62,63]. The high number of seismic events registered is related with the 2005 seismic crisis that affected the central part of São Miguel Island (Fogo/Congro area) and that had an increase number of seismic events in September 2005 [64]. Even if some residual values fall outside the variability band, it does not justify the identification of a direct relation between these two variables (Appendix A, Fig. A3). The multivariate regression analysis applied to the data acquired on the sampling point 2- Furnas Village Fumarolic Field did not had as objective to build a model, so the residuals were not calculated; for this reason, the raw soil ^{222}Rn concentration data were used in this analysis. During the period between 23rd January and 29th February 2009, on Furnas Volcano, 16 seismic events were recorded with duration magnitudes (Md) that varied between 0.8 and 2.0 (CVARG/CIVISA, http://www.cvarg.azores.gov.pt/paginas/sismicidade.aspx). The analysis of the residuals and the magnitudes of the seismic events do not justify the identification of a relation between these two variables (Appendix A, Fig. A4). During the measurements performed between 20th January 2009 and 1st February 2011, on sampling point 3- Furnas Village Fumarolic Field, 162 seismic events were recorded on the studied area with duration magnitudes (Md) that oscillated between 0.4 and 2.7 (CVARG/CIVISA, http://www.cvarg.azores.gov.pt/paginas/sismicidade.aspx). The analysis of the residuals and the magnitudes of the seismic events did not allow to identify a direct relation between these two variables also in this sampling point, even if there are some periods with increases in the ^{222}Rn data that coincide with occurrence of seismic events (Appendix A, Fig. A5).

8 Discussion and summary

Spectral analysis allowed to identify diurnal (wet period) and seasonal variations on sampling point 3. Air temperature, relative air humidity and wind speed are the variables that show correlation with soil ^{222}Rn concentration diurnal variations. Soil ^{222}Rn concentration minimum values are observed around noon, between 12:00 and 15:00, and maximum values are observed during the night, between 24:00 and 03:00. Soil ^{222}Rn concentration shows an inverse relation with air temperature (Fig. 8b) and wind speed (Fig. 4d). In fact, wind speed diurnal variations are approximately in phase with air temperature diurnal cyclic variations, due to the regular periodic changes in the atmospheric stability related with the increase in temperature (solar heating). During the night, when air temperature reaches the minimum values, an increase in the planetary boundary layer stability is observed and, as result, soil ^{222}Rn concentration increases. On another hand, during the day, due to solar heating, an increase on the instability of the planetary boundary layer is observed, leading to a downward turbulent mixing that contributes to the maximum wind speed in the afternoon and, as result, to a soil ^{222}Rn concentration decrease [65,66]. Soil ^{222}Rn concentration shows a time delay of about 3 hours with relative air humidity. A similar behaviour, one cycle per day variations on soil ^{222}Rn time series, was also observed on other volcanic areas in the Azores, such as Pico Alto, Terceira Island [67], and on granitic areas in Israel [68] and on geothermal areas in Nepal [69].

Table 2. Main frequencies identified in the soil ^{222}Rn concentration time series on wet period, on sampling point 3, and global phenomena with similar periodicity [70–72].

Periodicity (days)	Global phenomena with similar periodicity
∼340	Annual cycle – Earth translation movement (∼365 days)
∼48	Solar cycle (multiple of solar rotation ∼26 days)
∼25	Solar cycle (∼26 days)
∼15	Semi-lunar cycle (∼14 days)
∼1	Earth tides – diurnal cycle (24 h)

The low frequency analysis allowed to identify an annual cycle with approximately 340 days (Appendix A, Fig. A2). The difference observed between the annual cycle identified (340 days) and the 365 days associated with the annual cycle related with the Earth translation movement (Table 2), can result from the short sampling period (less than two years) that just allows one complete annual cycle. A longer time series (several years) should allow an approximation between the number of days on the observed annual cycle and the annual cycle related with the Earth translation movement, as suggested in previous works related with soil CO_2 flux [48]. Cycles of 48, 25 and 15 days were also identified (Appendix A, Fig. A2). The 48 and 25 days cycles are probably related with the solar cycle and the 15 days cycle can be related with the semi-lunar cycle (Table 2) [70–72]. 25 days is also within the period defined by Viveiros et al. [48] to this monitoring site for soil CO_2 flux time series. A cyclic behaviour on soil ^{222}Rn variation related with the lunar cycle was also observed on other volcanic regions, such as Stromboli Volcano [28] and Pico Alto Volcano [68].

The multivariate regression analysis applied to the different groups of soil ^{222}Rn concentration identified in each one of the different sampling points allowed to identify soil temperature, soil water content, barometric pressure, wind speed, relative air humidity, air temperature and soil CO_2 flux as the statistical meaningful variables. The set of variables that influence soil ^{222}Rn concentration on the same group of the various sampling points is different, and even on the same sampling point the set of variables is also different for each one of the groups identified. On another hand, common variables can have a different type of influence on the different groups of data (positive, negative or a second-order polynomial behaviour) (Table 3).

The models applied to the groups of data identified as "A" (A1, A2 and A3) allow to identify soil temperature as the common independent variable (Table 3). Soil temperature shows a negative correlation with the ^{222}Rn data of the group A1 and a positive correlation with the data of the groups A2 and A3. The difference in the signal of the influence observed can be related with the fact that the sampling point 1 is located in an area without soil thermal anomaly, while the sampling points 2 and 3 are located in the vicinity of fumarolic fields in areas with thermal anomalies (Appendix B, Table B2). This behaviour results from the fact that an increase on soil temperature conducts to an enhance of ^{222}Rn emanation power and transport to the surface [11,50]. Soil temperature is the independent variable with more explanatory power (Table 3) in the models of the groups A2 and A3. The datasets identified as groups "A" of data represent the low soil ^{222}Rn concentration values and can be explained or by seasonal variations (as observed, for instance, in figure 3 c) and d), lower ^{222}Rn values are recorded during "winter" months), or by some technical problems in the equipment that was not possible to identify. However, technical problems are discharged for group A3 since: a) low ^{222}Rn values are observed for a long period of time (months), b) the model have an explanatory power of 27% and a high number

Table 3. Comparison of the multivariate regression results for the three groups of data at the sampling points: A ($< 8000\,\mathrm{Bq/m^3}$), B ($8000 <$ B1 $< 16000\,\mathrm{Bq/m^3}$, ($8000 <$ B3 $< 50000\,\mathrm{Bq/m^3}$) and C (C1 and C2 $> 16000\,\mathrm{Bq/m^3}$, C3 $> 50000\,\mathrm{Bq/m^3}$).

	1-Furnas Thermal Centre			2-Furnas Village Fumarolic Field			3-Furnas Lake Fumarolic Field		
	Variables	Influence	Explanatory power	Variables	Influence	Explanatory power	Variables	Influence	Explanatory power
A	Soil water content	–	12.6%	Soil temperature	+	50.5%	Soil temperature	+	17.6%
	Soil temperature	–	3.2%	Soil water content	+	7.1%	Wind speed	–	6.5%
				Wind speed	+	3.9%	Relative air humidity	+	1.7%
							Soil CO_2 flux	+	1.2%
Total			15.8%			61.5%			27%
B	Barometric pressure	–	32.3%	Not enough number of observations			Wind speed	–	7.7%
	$(\text{Soil temperature})^2$	–	31%				Relative air humidity	–	4.3%
	Soil water content	+	4.7%						
	$(\text{Soil water content})^2$	–	3.8%						
	Soil temperature	+	1.8%						
Total			73.6%						12%
C	Soil water content	+	19.1%	Barometric pressure	+	51%	$(\text{Soil temperature})^2$	+	20.9%
	Soil CO_2 flux	+	15.8%	Air temperature	+	6.8%	Soil water content	+	18.8%
	$(\text{Soil temperature})^2$	–	4.2%				Soil CO_2 flux	+	6.5%
	Soil temperature	+	1.4%				Soil temperature	–	4.2%
Total			40.5%			57.8%			50.4%

of observations ($n = 8994$), c) soil CO_2 flux has a positive influence on the soil ^{222}Rn concentration, indicating that this gas can act as a carrier transporting ^{222}Rn until the surface [39,43], and d) the data show a seasonal variation, with higher values during the "summer" period and lower values in "winter" (Fig. 3d). The soil ^{222}Rn concentration seasonal variation can be correlated with the soil temperature and soil water content seasonal variation. The increase on soil temperature during the summer period can promote an increase on the release of ^{222}Rn from the soil and rocks, which, combined with the decrease on the soil water content promotes a faster and more efficient transport until the surface. On another hand, the seasonal variation observed can also be associated with changes on the water table level due to the proximity of the sampling point 3 to Furnas Lake. A similar behaviour was observed on some fault zones where the water table changes and the presence of water is also responsible for a clear seasonal effect with important decreases on the ^{222}Rn values during the winter/wet periods [73,74]. Values identified as group "A" (≤ 8000 Bq/m^3) represent the lowest soil ^{222}Rn concentrations recorded in the three monitoring sites and are all within the background defined by Silva [10] for ^{222}Rn concentration at Furnas Volcano (≤ 8000 Bq/m^3), considering the spatial distribution of the data.

The models applied to the groups "B" (B1 and B3), which represent the intermediate soil ^{222}Rn concentration values, allowed to verify that these groups of data were exclusively influenced by meteorological variables (Table 3) and no common independent variable was identified.

The models applied to the groups identified as "C" (C1, C2 and C3) allowed identifying soil water content, soil temperature and soil CO_2 flux as the common independent variables to the models of C1 and C3 groups (Table 3). Soil water content shows a positive correlation with the ^{222}Rn data on both groups. Soil temperature has a second-order polynomial function behaviour and shows a negative influence on the C1 model and a positive influence on the C3 model above the respective stationary points. As observed in the data of the groups "A", soil temperature shows a different influence in the groups of data C1 and C3 (Table 3) that is also probably related with the fact that the sampling point is located, or not, in a soil temperature anomalous zone. Group "C" values correspond to the highest ^{222}Rn records and are probably associated with the presence of a carrier gas (in this case, the CO_2), specially at monitoring sites 1 and 3, which is supported by the fact that soil CO_2 flux shows a positive correlation with the ^{222}Rn data of the groups C1 and C3.

On sampling point 1 (A1, B1 and C1), the models applied allow to identify soil water content and soil temperature as the common independent variables (Table 3). Soil water content has a complex influence on the different groups of data. This variable has a second-order polynomial behaviour on the group of data B1, changing its influence on the ^{222}Rn gas from positive to negative at the stationary point. The positive influence of soil water content can be interpreted as blocking of soil pores on shallow levels due to the presence of water, what conducts to an increase on soil ^{222}Rn concentration on the sampling point ($\sim$60 cm depth). The negative influence probably results from intense rainfall periods that conduct to ^{222}Rn dissolution and transport to deeper layers, not allowing its detection [75]. Soil water content shows a negative influence on the data of the group A1. This behaviour can be the result, as described above, of ^{222}Rn dissolution and transport to deeper layers and/or can be also related with the low ^{222}Rn values of this group of data ($^{222}Rn \leq 8000$ Bq/m^3). Soil water content has a positive influence on the data of the group C1; this influence should result from the impermeability of the shallow levels due to the presence of water (rainfall), conducting to an increase of soil ^{222}Rn concentration at the sampling point. Previous studies showed also the important influence of soil water content and soil temperature in the variation of soil CO_2 flux in this monitoring site [47].

The data of the group B1 also shows a negative correlation with barometric pressure. A decrease in the barometric pressure results on an increase on soil ^{222}Rn concentration due to a decrease on the pressure near the soil surface that allows a vertical transport of ^{222}Rn present at deeper layer ("pumping effect"). On another hand, an increase of barometric pressure forces ^{222}Rn to deeper layers conducting to a decrease on soil ^{222}Rn concentration measured at the sampling point [73,76].

On sampling point 2, no common independent variables were identified on the different groups (Table 3). On sampling point 3, wind speed and relative air humidity are the common independent variables on the models of the groups A3 and B3 (Table 3). Wind speed has a negative influence on both groups of data and probably is consequence of the dilution of the ^{222}Rn present on the soil shallower levels [33]. Negative influence of wind speed on soil CO_2 flux variations was also identified in previous works in this monitoring site [47]. Relative air humidity shows a positive influence on the group A3, since high relative air humidity values inhibited ^{222}Rn exhalation from soil to the atmosphere conducting to an increased on the soil ^{222}Rn concentration on the sampling point [77]. However, on the group B3, this variable has a negative influence that can be the result of the superimposed influence of another variable.

Soil temperature and soil CO_2 flux are the common independent variables to the models of the groups A3 and C3 (Table 3). Soil temperature shows a positive correlation with soil ^{222}Rn concentration on the group of data A3, and a second-order polynomial behaviour on C3. Soil CO_2 flux has a positive influence on both groups of data.

This work shows for the first time combined statistical analyses (multivariate regression coupled with spectral analysis) applied to soil ^{222}Rn concentration time series recorded in a quiescent volcanic area and thus may constitute powerful tools applied in any seismovolcanic monitoring system. These methodologies may allow identifying anomalies related with deep processes (e.g., seismic events or magmatic intrusions), and even if no reactivation was identified at Furnas volcanic system during the period under analyses, statistical analyses applied to the data allowed to define baseline behaviour for ^{222}Rn concentration and identify various environmental variables that can interfere with ^{222}Rn variations.

In addition, and taking into account that a) at Furnas Volcano there are two villages, b) ^{222}Rn is a radioactive gas, and c) soil is the main indoor ^{222}Rn source, understand the influence of external parameters on soil ^{222}Rn concentration is also important to try to recognize how the indoor ^{222}Rn concentration will change in function of soil ^{222}Rn concentration variation.

The authors would like to thank Dr. José Cabral Vieira for his suggestions and discussion about multivariate regression analysis. Suggestions of Dr. Gideon Steinitz and two anonymous reviewers also contributed to improve an early version of this manuscript. C. Silva and F. Viveiros were supported by Doctoral and Post Doctoral grants from Fundo Regional da Ciência e Tecnologia, Região Autónoma dos Açores (PROEMPREGO Operational Program).

Appendix A

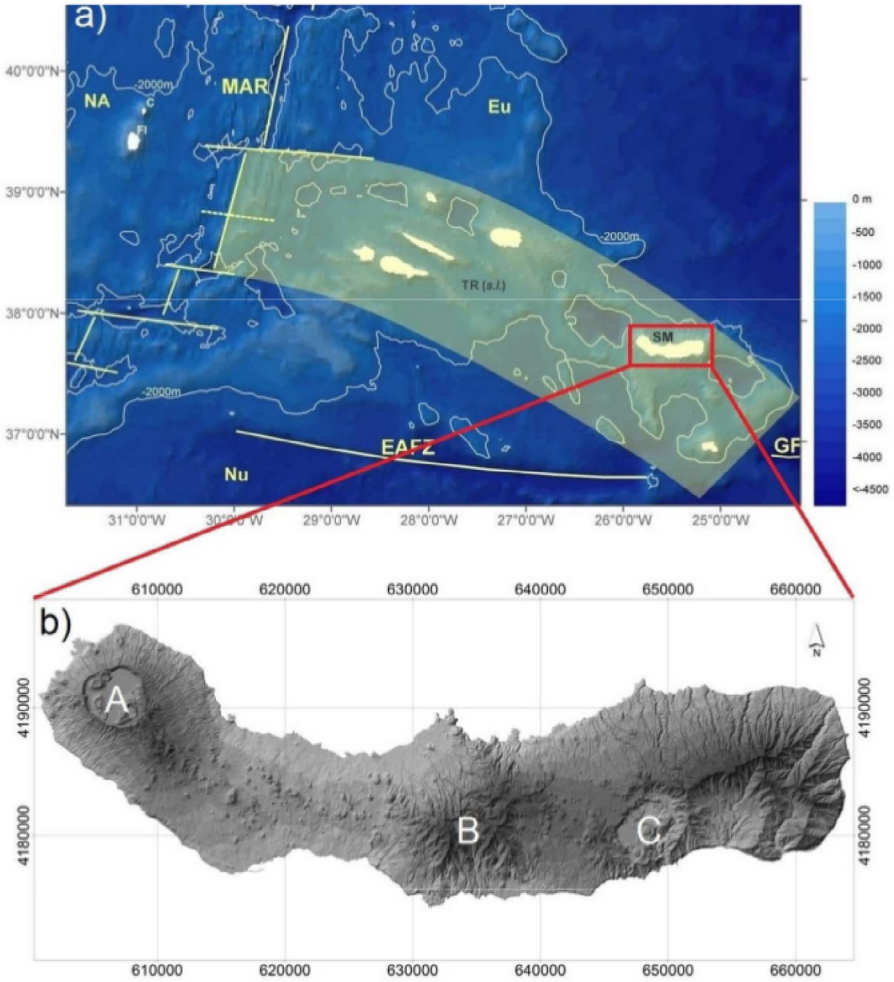

Fig. A1. Geological setting of the Azores archipelago and Furnas Volcano location: a) Azores archipelago located on the triple junction: NA- North American, Eu- Eurasian, Nu- Nubian (African) tectonic plates; and main tectonic structures: MAR- Mid-Atlantic Ridge, EAFZ- East Azores Fracture Zone, GF- Gloria Fault, and TR- Terceira Rift [78 and references therein]; b) São Miguel Island elevation model with the location of the active central volcanoes: A- Sete Cidades, B- Fogo and C- Furnas.

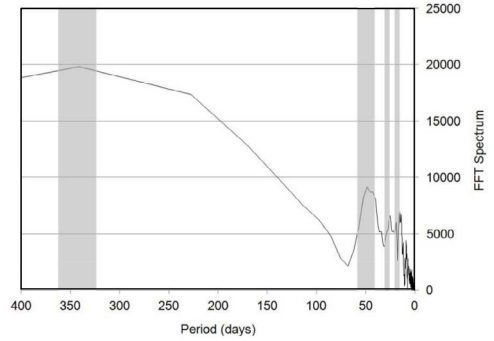

Fig. A2. Amplitude spectrum highlighting the low frequency of soil ^{222}Rn concentration on the sampling point 3- Furnas Lake Fumarolic Field. Grey shadows highlight 340, 48, 25 and 15 days peaks.

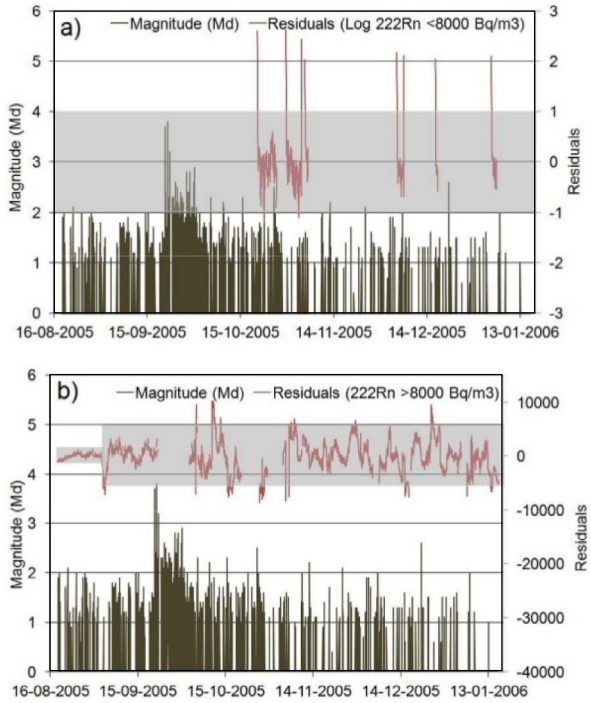

Fig. A3. Magnitude (Md) of seismic events and residuals temporal variation on the sampling point 1- Furnas Thermal Center: a) group of data A1, and b) groups of data B1 and C1. Grey band represents the $\mu \pm 2\sigma$ interval.

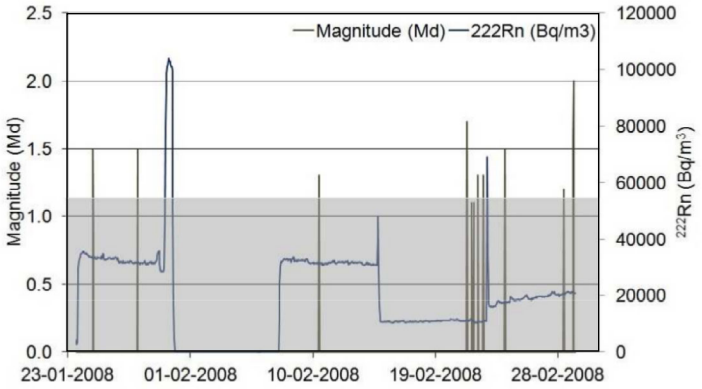

Fig. A4. Magnitude of seismic events and soil ^{222}Rn concentration temporal variation on the sampling point 2 – Furnas Village Fumarolic Field. Grey band represents the $\mu \pm 2\sigma$ interval.

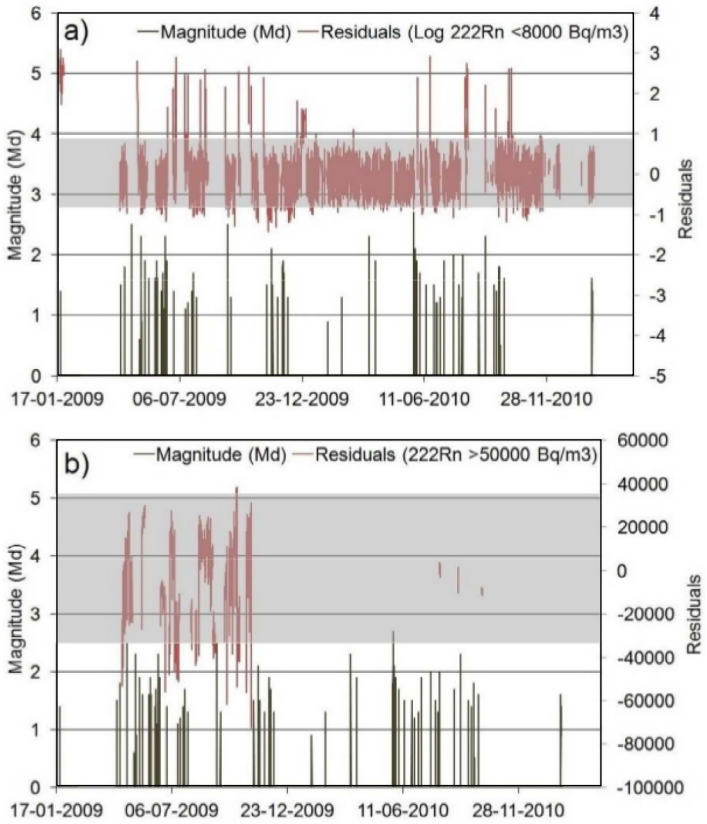

Fig. A5. Magnitude (Md) of seismic events and residuals temporal variation on the sampling point 3 – Furnas Lake Fumarolic Field: a) group of data A3, and b) groups of data B3 and C3. Grey band represents the $\mu \pm 2\sigma$ interval.

Appendix B

Table B1. Technical characteristics of the sensors installed in the permanent stations GFUR1, GFUR2[a] and GFUR3.

Parameters	Sensor type	Range and accuracy
CO_2 concentration	DRÄGER Polytron IR CO2	0–100% (configurable by the operator)
Soil temperature	Pt 100 Thermometer	0–200°C (±0.3°C)
Soil water content	CS616 Reflectometer	5–50% (±3%)
Barometric pressure	PT100B Pressure Transducer	600–1060 hPa (±0.5 hPa)
Rain	LASTEM Rain gauge	Unlimited (resolution: 0.2 mm)
Wind speed and direction	LASTEM Gonio-anemometer	0–60 m/s (±1%); 0–359.9°N (±0.5°)
	Gill sonic wind sensor[a]	0–60 m/s (±4%); 0–359.9 °N (±3°)
Relative air humidity and air temperature	Thermo-hygrometer	0–100%(±1%); −30 to 70 °C (±0.1 °C)

Table B2. Descriptive statistics of soil ^{222}Rn concentration, soil CO_2 flux and soil temperature data on the sampling points and considering the different groups.

Sampling point	Group of data	Variables	Average	Standard deviation	Median	Minimum	Maximum	Number of data
1	Total	^{222}Rn (Bq/m^3)	19558	8816	22100	0	39200	3363
		Soil CO_2 flux (g/m^{2}d)	286.7	70.4	278.2	1.7	1105.7	3621
		Soil temperature (°C)	18.9	2.3	18.4	15.2	22.7	3618
	A1	^{222}Rn (Bq/m^3)	176	897	19	0	7790	417
		Soil CO_2 flux (g/m^{2}d)	302.8	84.6	293.3	164.7	993.8	417
		Soil temperature (°C)	18.7	1.5	18.9	16.1	20.4	417
	B1	^{222}Rn (Bq/m^3)	12625	1464	12300	8330	16000	412
		Soil CO_2 flux (g/m^{2}d)	275.3	66.7	270.1	2.2	443.4	412
		Soil temperature (°C)	21.3	1.3	21.8	16.1	22.2	374
	C1	^{222}Rn (Bq/m^3)	23874	3790	23500	16100	39200	2534
		Soil CO_2 flux (g/m^{2}d)	292.6	69.2	285.3	20.6	1105.5	2534
		Soil temperature (°C)	18.3	2.2	17.7	15.2	22.7	2498
2	Total	^{222}Rn (Bq/m^3)	19535	16030	18900	33	104000	884
		Soil CO_2 flux (g/m^{2}d)	509	202.4	531.1	2	1138.3	880
		Soil temperature (°C)	27.8	1	27.5	26.8	30.3	357
	A2	^{222}Rn (Bq/m^3)	173	546	86	33	4580	188
		Soil CO_2 flux (g/m^{2}d)	360.6	161.6	419.9	2	633.5	187
		Soil temperature (°C)	27.1	0.5	27.0	26.8	30.3	188
	B2	^{222}Rn (Bq/m^3)	11044	858	10900	10300	16000	194
		Soil CO_2 flux (g/m^{2}d)	690.6	97.3	677.1	503.8	1138.3	194
		Soil temperature (°C)						0
	C2	^{222}Rn (Bq/m^3)	30067	13144	31500	16100	33400	502
		Soil CO_2 flux (g/m^{2}d)	493.8	194.3	527.9	30.8	849.8	499
		Soil temperature (°C)	28.6	0.8	28.4	27.2	30.3	169
3	Total	^{222}Rn (Bq/m^3)	19297	39672	17	0	153000	13321
		Soil CO_2 flux (g/m^{2}d)	393.9	95.6	397.8	11.7	774.2	15004
		Soil temperature (°C)	21.2	4.6	22.1	12.1	29.8	15726
	A3	^{222}Rn (Bq/m^3)	84	562	11	0	8000	10311
		Soil CO_2 flux (g/m^{2}d)	403	96.7	405.8	12.5	773.5	9938
		Soil temperature (°C)	20.7	4.5	21.8	12.1	29.7	10058
	B3	^{222}Rn (Bq/m^3)	27516	12905	26050	8290	50000	590
		Soil CO_2 flux (g/m^{2}d)	323.9	88.9	308.1	35.5	528.9	433
		Soil temperature (°C)	21.7	2.7	22.5	17.6	29.7	435
	C3	^{222}Rn (Bq/m^3)	99159	25585	101000	50200	153000	2420
		Soil CO_2 flux (g/m^{2}d)	403.9	60.4	411.1	110.4	611.6	2230
		Soil temperature (°C)	25.9	2.5	27	18.9	29.8	2279

Table B3. Multivariate regression analysis applied to the three groups of data at the sampling point 1.

Group of data	Independent variable	Coefficient B	Standard error of B	Coefficient β	t test	Adjusted R^2 increase	VIF
A1	Intercept	4.07	0.34		12.09		
	Soil water content	−0.08	0.01	−0.29	−6.01	0.126	1.14
	Soil temperature	−0.08	0.02	−0.02	−4.06	0.032	1.14
	Dependent variable: Log_{10} soil ^{222}Rn concentration ($\leq$8000 Bq/m3) Number of observations: 415 Adjusted R^2 sum: 0.158 F test: 832.85						
B1	Intercept	144631.1	17933.10		8.07		
	Barometric pressure	−209.94	9.39	−0.67	−22.37	0.323	1.28
	(Soil temperature)^2	−214.87	40.00	−7.32	−5.37	0.310	2614.00
	Soil water content	1998.03	224.84	3.56	8.89	0.047	226.22
	(Soil water content)^2	−92.07	9.01	−0.37	−10.22	0.038	181.18
	Soil temperature	1859.48	1566.1	6.75	5.02	0.018	2547.00
	Dependent variable: soil ^{222}Rn concentration (8000 to 16000 Bq/m^3) Number of observations: 373 Adjusted R^2 sum: 0.736 F test: 208.17						
C1	Intercept	−31700.94	5209.49		−6.09		
	Soil water content	893.71	32.84	0.43	27.21	0.191	1.03
	Soil CO_2 flux	365.03	15.62	0.39	23.38	0.158	1.15
	(Soil temperature)^2	−122.27	14.82	−2.73	−8.25	0.042	458.86
	Soil temperature	4249.67	559.2	2.51	7.6	0.014	458.19
	Dependent variable: soil ^{222}Rn concentration (> 16000 Bq/m^3) Number of observations: 2495 Adjusted R^2 sum: 0.405 F test: 347.51						

Table B4. Multivariate regression analysis applied to the three groups of data at the sampling point 2.

Group of data	Independent variable	Coefficient B	Standard error of B	Coefficient β	t test	Adjusted R^2 increase	VIF
A2	Intercept	−12.64	1.09		−13.55		
	Soil temperature	0.57	0.04	0.92	15.49	0.505	1.46
	Soil water content	0.09	0.02	0.29	5.68	0.071	1.1
	Wind speed	0.01	0.00	0.23	4.09	0.039	1.35
	Dependent variable: $\mathrm{Log_{10}}$ soil ^{222}Rn concentration ($\leq$8000 Bq/m^3) Number of observations: 161 Adjusted R^2 sum: 0.615 F test: 86.03						
C2	Intercept	−4246000.00	319425.84		−13.29		
	Barometric pressure	4230.68	317.57	0.71	13.32	0.510	1.00
	Air temperature	1131.43	225.61	0.27	5.02	0.068	1.00
	Dependent variable: soil ^{222}Rn concentration ($>$ 16000 Bq/m^3) Number of observations: 152 Adjusted R^2 sum: 0.578 F test: 104.39						

Table B5. Multivariate regression analysis applied to the three groups of data at the sampling point 3.

Group of data	Independent variable	Coefficient B	Standard error of B	Coefficient β	t test	Adjusted R^2 increase	VIF
A3	Intercept	−0.44	0.05		−8.26		
	Soil temperature	0.04	0.00	0.34	35.75	0.176	1.14
	Wind speed	−0.13	0.01	−0.23	−23.97	0.065	1.11
	Relative air humidity	0.01	0.00	0.13	14.62	0.017	1.03
	Soil CO_2 flux	0.01	0.00	0.12	12.40	0.012	1.10
	Dependent variable: Log_{10} soil ^{222}Rn concentration ($\leq$8000 Bq/m^3) Number of observations: 8994 Adjusted R^2 sum: 0.270 F test: 832.85						
B3	Intercept	57467.06	4839.32		11.98		
	Wind speed	−3215.16	574.64	−0.28	−5.6	0.077	1.00
	Relative air humidity	−246.12	56.97	−0.21	−4.32	0.043	1.00
	Dependent variable: soil ^{222}Rn concentration (8000 to 50000 Bq/m^3) Number of observations: 363 Adjusted R^2 sum: 0.120 F test: 25.64						
C3	Intercept	1122000	63947.5		17.55		
	(Soil temperature)^2	1972.03	101.69	10.11	19.39	0.209	1223.00
	Soil water content	4049.44	100.11	0.75	40.45	0.188	1.56
	Soil CO_2 flux	2317.11	134.92	0.28	17.18	0.065	1.21
	Soil temperature	−95386.87	5188.76	−9.51	−18.38	0.042	1204.00
	Dependent variable: soil ^{222}Rn concentration (> 50000 Bq/m^3) Number of observations: 2231 Adjusted R^2 sum: 0.504 F test: 568.457						

References

1. G. Queiroz, J.L. Gaspar, P.D. Cole, J.E. Guest, N. Wallenstein, A.M. Duncan, J. Pacheco, Açoreana **VIII**, 159 (1995)
2. J.E. Guest, J.L. Gaspar, P.D. Cole, G. Queiroz, A.M. Duncan, N. Wallenstein, T. Ferreira, J.M. Pacheco, J. Volcanol. Geotherm. Res. **92**, 1 (1999)
3. J.V. Cruz, R.M. Coutinho, M.R. Carvalho, N. Oskarsson, S.R. Gislason, J. Volcanol. Geotherm. Res. **92**, 151 (1999)
4. T. Ferreira, N. Oskarsson, J. Volcanol. Geotherm. Res. **92**, 169 (1999)
5. F. Viveiros, C. Cardellini, T. Ferreira, S. Caliro, G. Chiodini, C. Silva, J. Geophys. Res. **115**, B12208 (2010)
6. F. Viveiros, Ph.D. thesis, University of the Azores, 2010
7. J.C. Baubron, P.J. Baxter, R. Coutinho, P. Allard, T. Ferreira, J.L. Gaspar in *Proceedings of the European laboratory Volcanoes Workshop*, Catania, 1994, edited by F. Barberi, R. Casale, M. Fratta (European Comission DG XII, European Science Foundation, 1994), p. 262
8. F. Sousa, Master thesis, University of the Azores, 2003
9. C. Silva, Master thesis, University of the Azores, 2006
10. C. Silva, Ph.D. thesis, University of the Azores, 2013
11. M.E. Cox, Master thesis, University of Hawaii, 1980
12. D.M. Thomas, K.E. Cuff, M.E. Cox, J. Geophys. Res. **91**, 12186 (1986)
13. C. Connor, B. Hill, P. Lafemina, M. Navarro, M. Conway, J. Volcanol. Geotherm. Res. **73**, 119 (1996)
14. M. Heiligmann, J. Stix, G. Williams-Jones, B.S. Lollar, G. Garzón, J. Volcanol. Geotherm. Res. **77**, 267 (1997)
15. N. Segovia, M. Mena, P. Peña, E. Tamez, J.L. Seidel, M. Monnin, C. Valdez, Radiat. Meas. **31**, 307 (1999)
16. N. Segovia, C. Valdez, P. Peña, M. Mena, E. Tamez, Radiat. Meas. **34**, 433 (2001)
17. M.A. Armienta, N. Varley, E. Ramos, Geofísica Internacional **41**, 271 (2002)
18. S. Alparone, B. Bhncke, S. Giammanco, M. Neri, P. Privitera, Geophys. Res. Lett. **32**, L16307 (2005)
19. G. Immè, S. La Delfa, S. Lo Nigro, D. Morelli, G. Patanè, Ann. Geophys. **48**, 65 (2005)
20. G. Immè, S. La Delfa, S. Lo Nigro, D. Morelli, G. Patanè, Radiat. Meas. **41**, 241 (2006)
21. G. Immè, S. La Delfa, S. Lo Nigro, D. Morelli, G. Patanè, Appl. Radiat. Isot. **64**, 624 (2006)
22. D. Morelli, S. Di Martino, G. Immè, S. La Delfa, S. Lo Nigro, G. Patanè, Radiat. Meas. **41**, 721 (2006)
23. M. Neri, B. Bechncke, M. Burton, G. Galli, S. Giammanco, E. Pecora, E. Privitera, D. Reitano, Geophys. Res. Lett. **33**, L24316 (2006)
24. S. La Delfa, G. Immè, S. Lo Nigro, D. Morelli, G. Patanè, F. Vizzini, Radiat. Meas. **42**, 1404 (2007)
25. S. La Delfa, I. Agostino, D. Morelli, G. Patanè, Radiat. Meas. **43**, 1299 (2008)
26. C. Cigolini, G. Gervino, R. Bonetti, F. Conte, M. Laiolo, D. Coppola, A. Manzoni, Geophys. Res. Lett. **32**, L12308 (2005)
27. C. Cigolini, M. Laiolo, D. Coppola, Earth Planet. Sci. Lett. **257**, 511 (2007)
28. C. Cigolini, P. Poggi, M. Ripepe, M. Laiolo, C. Ciamberlini, D. Delle Done, G. Ulivieri, D. Coppola, G. Lacanna, E. Marchetti, D. Piscopo, R. Genco, J. Volcanol. Geotherm. Res. **184**, 381 (2009)
29. M. Laiolo, C. Cigolini, D. Coppola, D. Piscopo, J. Environ. Radioact. **105**, 21 (2012)
30. P. Delmelle, J. Stix, in *Encyclopedia of Volcanoes*, edited by H. Sigurdsson, B. Houghton, S.R. McNutt, H. Rymer, J. Stix (American Press, 2000)
31. C.-Y. King, J. Geophys. Res. **85**, 3065 (1980)
32. T.F. Yang, V. Walia, L.L. Chyi, C.C. Fu, C.-H. Chen, T.K. Liu, S.R. Song, C.Y. Lee, M. Lee, Radiat. Meas. **40**, 496 (2005)
33. A. Kumar, S. Sing, S. Mahajan, B.S. Bajwa, R. Kalia, S. Dhar, Appl. Radiat. Isot. **67**, 1904 (2009)

34. C. Papastefanou, Radiat. Meas. **45**, 943 (2010)
35. D.V. Reddy, P. Nagabhushanam, Appl. Geochem. **26**, 731 (2011)
36. A.M. Chirkov, Bull. Volcanol. **39**, 126 (1975)
37. J.C. Baubron, P. Allard, J.P. Toutain, Nature **344**, 51 (1990)
38. J.C. Baubron, P. Allard, J.C. Sabroux, D. Tedesco, J.P. Toutain, J. Geol. Soc. Lond. **148**, 571 (1991)
39. G. Etiope, S. Lombardi, J. Radioanal. Nucl. Chem. **193**, 291 (1995)
40. G. Ciotoli, G. Etiope, M. Guerra, S. Lombardi, Tectonophysics **301**, 321 (1999)
41. G. Ciotoli, S. Lombardi, A. Annunziatellis, J. Geophys. Res. **112**, B05407 (2007)
42. M. Guerra, S. Lombardi, Tectonophysics **339**, 511 (2001)
43. G. Etiope, G. Martinelli, Phys. Earth and Planet. Int. **129**, 185 (2002)
44. P. Allard, J. Carbonnelle, D. Dajlevic, J. Le Bronec, P. Morel, M.C., Robe, J.M. Maurenas, R. Faivre-Pierret, D. Martin, J.C. Sabroux, P. Zettwoog, Nature **351**, 387 (1991)
45. G. Chiodini, R. Cioni, M. Guidi, B. Raco, L. Marini, Appl. Geochem. **13**, 543 (1998)
46. G. Williams-Jones, H. Rymer, in *Encyclopedia of Volcanoes*, edited by H. Sigurdsson, B. Houghton, S.R. McNutt, H. Rymer, J. Stix (American Press, 2000)
47. F. Viveiros, T. Ferreira, J.C. Vieira, C. Silva, J.L. Gaspar, J. Volcanol. Geotherm. Res. **177**, 883 (2008)
48. F. Viveiros, J. Vandemeulebrouck, A.P. Rinaldi, T. Ferreira, C. Silva, J.V. Cruz, J. Geophys. Res. Solid Earth **119**, 7578 (2014)
49. A.P. Rinaldi, J. Vandemeulebrouck, M. Todesco, F. Viveiros, J. Geophys. Res. **117**, B11201 (2012)
50. P. Gasparini, M.S.M. Mantovani, J. Volcanol. and Geotherm. Res. **3**, 325 (1978)
51. J.C. Baubron, A. Rigo, J.P. Toutain, Earth Planet. Sci. Lett. **196**, 69 (2002)
52. M. Van Camp, P. Vauterin, Computers Geosci. **31**, 631 (2005)
53. P. Vauterin, M. Van Camp, Tsoft Manual (Royal Observatory of Belgium, Bruxelles, 2011)
54. F.J. Harris, Proceedings of the IEEE **66**, 51 (1978)
55. N. Draper, H. Smith, *Applied Regression Analysis*, 2nd edn. (John Wiley and Sons, Inc., USA, 1981)
56. R.J. Freund, W.J. Wilson, *Regression analysis. Statistical modeling of a response variable* (Academic Press., USA, 1998)
57. J.L. Gaspar, T. Ferreira, G. Queiroz, N. Wallenstein, J. Pacheco, J. Guest, A. Duncan, P. Cole, Universidade do Porto – Faculdade de Ciências Museu e Laboratório Mineralógico e Geológico **4**, 999 (1995)
58. C. Carmo, Master thesis, University of the Azores, 2004
59. R. Marques, J. Zêzere, R. Trigo, J.L. Gaspar, I. Trigo, Hydrol. Process. **22**, 478 (2008)
60. J. Planinic, V. Radolic, Z. Lazanin, Appl. Radiat. Isot. **55**, 267 (2001)
61. I. Miklavcic, V. Radolic, B. Vukovic, M. Poje, M. Varga, D. Stanic, J. Planinic, Appl. Radiat. Isot. **66**, 1459 (2008)
62. W. Lee, R. Bennet, K. Meagher, U.S. Geological Survey, Open File Report (1972)
63. J. Wellik II, Master thesis, Michigan Technological University, 2014
64. R. Silva, J. Havskov, C. Bean, N. Wallenstein, J. Seismol. **16**, 389 (2012)
65. A. Dai, C. Desser, J. Geophys. Res. **104**, 31109 (1999)
66. K. Singh, M. Singh, S. Singh, H.S. Sahota, Z. Papp, Radiat. Meas. **39**, 213 (2005)
67. F. Aumento, Geofísica Internacional **41**, 499 (2002)
68. G. Steinitz, O. Piatibratova, S.M. Barbosa, J. Geophys. Res. **112**, B10211 (2007)
69. P. Richon, F. Perrier, B.P. Koirala, F. Girault, M. Bhattarai, S.N. Sapkota, J. Environ. Radioact. **102**, 88 (2011)
70. Y. Han, Y. Han, Chin. Sci. Bull. **47**, 1969 (2002)
71. C.J. Groves-Kirkby, A.R. Denman, R.G.M. Crockett, P.S. Phillips, G.K. Gilmore, Sci. Total Environ. **367**, 191 (2006)
72. R.R. Schureman, U. S. Department of Commerce, Coast and Geodetic Survey, Special publication No. 98 (1976)

73. J.L. Pinault, J.C. Baubron, J. Geophys. Res. **102**, 18101 (1997)
74. Ll. Font, C. Baixeras, V. Moreno, J. Bach, Radiat. Meas. **43**, S319 (2008)
75. J.R. Garcia-Vindas, M.M. Monnin, Radiat. Meas. **39**, 319 (2005)
76. W.E. Clements, M.H. Wilkening, J. Geophys. Res. **79**, 5025 (1974)
77. M. García-Talavera, B. Quintana, E. García-Díez, F. Fernández, Atmos. Environ. **35**, 221 (2001)
78. A. Hipólito, Master thesis, University of the Azores, 2009